PEGylated Nanoparticles Based on a Polyaspartamide. Preparation, Physico-Chemical Characterization, and Intracellular Uptake

Emanuela F. Craparo,[†] Gennara Cavallaro,[†] Maria L. Bondì,[‡] Delia Mandracchia,[†] and Gaetano Giammona*[,†]

Dipartimento di Chimica e Tecnologie Farmaceutiche, Università di Palermo, via Archirafi, 32-90123 Palermo, Italy, and Istituto per lo Studio dei Materiali Nanostrutturati, sez. di Palermo, Consiglio Nazionale delle Ricerche, Via Ugo la Malfa 153, 90146 Palermo, Italy

Received June 14, 2006; Revised Manuscript Received September 5, 2006

Nanoparticles with different surface PEGylation degree were prepared by using as starting material α,β-poly(*N*-2-hydroxyethyl)-D,L-aspartamide (PHEA). PHEA was functionalized with a PEG amino-derivative for obtaining PHEA-PEG_{2000} copolymer. Both PHEA and PHEA-PEG_{2000} were derivatized with methacrylic anhydride (MA) for obtaining poly(hydroxyethylaspartamide methacrylated) (PHM) and poly(hydroxyethylaspartamide methacrylated)-PEGylated (PHM-PEG_{2000}), respectively. Nanoparticles were obtained by UV irradiation of an inverse microemulsion, using as internal phase an aqueous solution of PHM alone or of the PHM/PHM-PEG_{2000} mixture at different weight ratio and as external phase a mixture of propylene carbonate and ethyl acetate. Obtained nanoparticles were characterized by FT-IR analysis, dimensional analysis, and TEM micrography. XPS analysis and zeta potential measurements demonstrated the presence of PEG onto the nanoparticle surface. Moreover, the partial degradation of nanoparticles in the presence of esterase as a function of time was demonstrated. Finally, nanoparticles did not possess any cytotoxic activity against K-562 cells and were able to escape from phagocytosis depending on the surface PEGylation degree.

Introduction

One of the most attractive research areas in drug delivery is the design of nanosystems (at polymeric and lipidic structure) being able to deliver drugs to the right place, at appropriate times.[1,2]

Nanoparticles are colloidal systems which have recently attracted great interest for clinical administration of several classes of drugs, thanks to many advantages rising from their submicron size, such as high capability to cross various physiological barriers, possible administration by all of the routes, and controlled and targeted delivery of the drug.[1,3]

Besides, physicochemical and structural properties such as size, surface charge, morphology, and the composition of the polymer matrix play a key role on their fate and can be easily optimized also to achieve proper drug release kinetics, biological activity and compatibility.[4]

Generally, after intravenous administration, nanoparticles are extensively taken up by the liver, spleen, and other parts of the reticulo-endothelial system (RES) depending on their size and surface characteristics. Coating of nanoparticles with opsonic materials such as gamma globulin, human fibronectin, and gelatin could enhance the phagocytosis by macrophages.[5] This strategy can be usefully exploited for obtaining drug targeting to macrophages, which play a important role in host defense against many infectious agents and tumor cells.[5] So, the delivery of drugs to macrophages can be an astute strategy for an efficacious treatment of both infectious and devastating diseases such as cancer.[5]

On the other hand, stealth nanoparticles, with longer circulation time and hence greater ability to reach the target site, can be realized by achieving very small particle size as well as coating surface nanoparticles with appropriate hydrophilic material in order to reduce uptake by macrophages and to prolong blood residence time.[3,6]

Poly(ethylene glycols) (PEGs) are widely used as coating material to obtain stealthy particles. The stable anchoring of the coating layer on the particle surface is an essential feature in modifying particle interaction with biological environment.

PEG chains can be physically adsorbed on or covalently linked to the particle surface. In both cases, PEG chains create an hydrophilic barrier layer to inhibit the adhesion of opsonins present in blood serum, so that the particles can remain camouflaged or invisible to phagocytic cells.[7] However, the use of surface adsorbed PEG moieties has the drawback that they could desorb once in the blood stream, leaving holes in surface coverage where opsonins can bind.[7]

Particles with covalently bound PEG chains achieve longer blood circulation half-lives than similar particles with only surface adsorbed PEG.[8] PEG moieties can be covalently bonded to fully formed nanoparticles by various techniques such as traditional surface functional group chemistry.[9] Another possibility is to prepare nanoparticles by using among starting materials PEG copolymer. As a result, covalently bounded PEG chains can be either exposed at the particle surface or incorporated throughout the bulk of the material with positive effects also on the degradation and erosion processes of nanoparticle matrixes.

Our research group has recently developed a new method for obtaining nanoparticles by UV irradiation of acryloylated copolymers.[10] UV− induced cross-linking of hydrophilic polymers represents a practical method for producing well-defined networks and provides significant advantages over conventional chemical cross-linking, such as the ease of production (the synthesis is carried out in a single step and without the presence of initiators), safety, and low cost.[11]

* To whom correspondence should be addressed. E-mail. gaegiamm@unipa.it. Telephone: 0039 091 6236128. Fax: 0039 091 6236150.

[†] Università di Palermo.

[‡] Consiglio Nazionale delle Ricerche.

10.1021/bm060570c CCC: $33.50
Published on Web 10/07/2006

In this paper, the preparation and characterization of stealth nanoparticles using as starting material a PEGylated copolymer is described.

In the first step of this work, α,β-poly(*N*-2-hydroxyethyl)-D,L-aspartamide (PHEA) was functionalized with a PEG amino derivative obtaining PHEA-PEG_{2000} copolymer. Both PHEA-PEG_{2000} and PHEA were subsequently derivatized with methacrylic anhydride (MA), obtaining two acryloylated copolymers called poly(hydroxyethylaspartamide methacrylated) (PHM) and poly(hydroxyethylaspartamide methacrylated)-PEGylated (PHM-PEG_{2000}), respectively.[12] Obtained acryloylated copolymers were able to cross-link by UV irradiation thanks to their improved reactivity to UV-rays due to the presence of double bonds in the polymeric structure. Moreover, the introduction in the copolymer structure of chemical residues having ester groups could provide potential biodegradability to the cross-linked matrixes.[13] Then, the preparation and characterization of polymeric nanoparticles with a different amount of covalently linked PEG was described. The X-ray photoelectron microscopy (XPS) analysis was used for estimating the efficiency of surface modification. Physicochemical and biological characterization of nanoparticles was also performed in terms of size, zeta potential, cytotoxicity, and cellular uptake.

Materials and Methods

Materials. All reagents were of analytical grade, unless otherwise stated. Ethanolamine, anhydrous *N*,*N*-dimethylformamide (DMF), anhydrous *N*,*N*-dimethylacetamide (DMA), propylene carbonate (PC), ethyl acetate (EtOAc), DMSO-d_6 and D_2O (isotopic purity 99.9%), pepsin from porcine stomach mucosa 3500 U (mg protein)$^{-1}$, α-chymotrypsin from bovine pancreas 49 U (mg protein)$^{-1}$, esterase from porcine liver 184 U (mg protein)$^{-1}$, and fluorescein sodium salt were purchased from Sigma-Aldrich (Italy). *O*-(2-Aminoethyl)-*O*′-methyl poly(ethylene glycol) 2000 (PEG_{2000}) (≤ 0.4 mmol NH_2/g), bis(4-nitrophenyl) carbonate (PNPC), methacrylic anhydride (MA), triethylamine (TEA), and block copolymer of polyethylene and polypropylene glycol (Synperonic PE/L61) were purchased from Fluka (Italy). Human chronic myelogenous leukemia cell line (K-562) and mouse monocyte macrophage cell line (J774 A.1) were purchased from Istituto Zooprofilattico Sperimentale della Lombardia e dell'Emilia Romagna "Bruno Umbertini" (Italy).

Apparatus. Molecular weights of PHEA, PHEA-PEG_{2000}, PHM, and PHM-PEG_{2000} were determined by a SEC system equipped with a pump system, two Phenogel columns from Phenomenex (5 μm particle size, 10^3 Å and 10^4 Å of pores size), and a 410 differential refractometer (DRI) as concentration detector, all from Waters (Mildford, MA). The molecular weights were determined by using PEO/PEG as standards (range 4000−318 000 Da), DMF + 0.01 M LiBr as mobile phase, a flow of 0.8 mL/min, and operating at 50 ± 0.1 °C.

^{1}H NMR spectra were obtained with a Bruker AC-250 instrument operating at 250.13 MHz.

UV irradiation was performed using a Rayonet reactor equipped with a Rayonet Carousel Motor Assembly and 16 mercury lamps of 8 W at low pressure with an emission at λ 254 nm.

Centrifugations were performed with an International Equipment Company Centra MP4R equipped with a 854 rotor and temperature control.

FT-IR spectra were taken in KBr pellets in the range 4000−400 cm^{-1} using a Perkin-Elmer 1720 Fourier transform spectrophotometer. The resolution was 1 cm^{-1}. The number of scans was 100. Spectra are recorded in transmittance scale (%*T*).

The size and zeta potential measurements were determined by a Zetasizer Nano ZS (Malvern Instrument, Herrenberg, Germany).

Transmission electron micrography (TEM) images were recorded on a Philips EM420 electron microscope at an accelerating voltage of 100 kV.

The X-ray photoelectron spectroscopy (XPS) analyses were performed with a VG Microtech ESCA 3000 Multilab spectrometer equipped with a standard Al K excitation source ($h\nu$ = 1486.6 eV) and a nine-channeltrons detection system.

The fluorescence microscopy images were viewed by a fluorescence microscope ZEISS-AXIO SKOP 2 PLUS with images captured using an AXIO camera HBO 100.

PHEA Synthesis. PHEA was prepared by reaction of a polysuccinimide (PSI) with ethanolamine in DMF solution, purified, and characterized according to a previously reported procedure.[14] The batch of PHEA used in the present study had a weight-average molecular weight ($\bar{M}_w$) of 36.4 kDa ($\bar{M}_w/\bar{M}_n$ = 1.82), determined by SEC analysis.

PHM Synthesis. The derivatization of PHEA with methacrylic anhydride to obtain PHM copolymer was carried out in anhydrous *N*,*N*-dimethylacetamide (DMA), by using TEA as catalyst, according to the before described procedure.[12] Briefly, PHEA (50 mg/mL) was dissolved in anhydrous DMA, and then a suitable amount of triethylamine (TEA) and methacrylic anhydride (MA) were added, according to R_1 = 0.5 and R_2 = 0.5, being

$$R_1 = \text{mol of MA/mol of PHEA repeating units}$$

$$R_2 = \text{mol of TEA/mol of MA}$$

The reaction was kept at 40 °C under continuous stirring for 48 h. After this time, the reaction mixture was precipitated in 2-propanol and centrifuged for 10 min, at 11 800 rpm and 4 °C. The product was recovered, washed five times with 2-propanol and 3 times with acetone, and then dried under vacuum.

PHM copolymer thus obtained was dissolved in twice-distilled water and subjected to extensive dialysis by using Visking Dialysis Tubing (18/32 in.) with a molecular weight cutoff of 12 000−14 000. After dialysis, the solution was dried by freeze-drying. PHM was obtained with a yield of 97−99 wt % based on the starting PHEA.

PHM copolymer was characterized as before reported.[12]

The degree of derivatization with methacrylic groups (DD_{MA}) was determined by ^{1}H NMR in D_2O and calculated by the following ratio:

$$DD_{MA} = \text{(methacrylic groups/polymer repeating units) x 100}$$

In particular, DD_{MA} was calculated by comparing the integral of the peaks related to protons at 1.9 δ as well as to protons between 5.71 and 6.12 δ respectively awardable to −CO−C(**CH_3**)=CH_2 and −CO−C(CH_3)=**CH_2** (belonging to linked MA) with the integral related to protons at 2.80 δ awardable to −CH−**CH_2**−CO−NH− (belonging to PHEA). The degree of derivatization was expressed as mean value of three determination and resulted to be 30 ± 1 mol %. The $\bar{M}_w$ of PHM copolymer determined by SEC measurements was 43 kDa ($\bar{M}_w/\bar{M}_n$ = 1.78).

PHEA-PEG_{2000} Synthesis. To a PHEA solution (40 mg/mL) in anhydrous DMF was added a proper amount of bis(4-nitrophenyl) carbonate (PNPC) in a such way as to have X = mol of PNPC/mol of PHEA repeating units equal to 0.1. The reaction mixture was kept at 40 °C for 2.5 h and then at 60 °C for 30 min. A solution of *O*-(2-aminoethyl)-*O*′-methyl poly(ethylene glycol) 2000 (PEG_{2000}) in anhydrous DMF (60.8 mg/mL) was then added to the mixture reaction in a such way as to have Y = mol of PEG_{2000}/mol of PNPC equal to 1.2 and the mixture left at 60 °C for 2.5 h under argon and continuous stirring.

After this time, the solution was precipitated in ethyl ether and washed three times with 50 mL aliquots of a mixture of ethyl ether/CH_2Cl_2 (2:1) and then five times with 50 mL aliquots of acetone. PHEA-PEG_{2000} copolymer thus obtained was dissolved in twice-distilled water and subjected to an extensive dialysis by using Visking Tubing Dialysis 18/32″ with a molecular weight cutoff of 12 000−14 000. After dialysis, the solution was dried by freeze-drying. The product was obtained with a yield of 95 wt % based on the starting PHEA.

FT-IR spectrum (KBr) of PHEA-PEG_{2000} showed a broad band centered at 3400 cm^{-1} (asymmetric stretching of O−H and N−H groups); bands at 2917 (stretching C−H); 1656 (amide I); 1543 (amide II) and 1110 cm^{-1} (stretching C−O).

^{1}H NMR spectrum (DMSO-d_6) of PHEA-PEG_{2000} showed: 2.6 (m, 2H, −CH−**CH_2**−CO−NH), 3.12 (t, 2H, −NH−**CH_2**−CH_2−O-), 3.35 (t, 2H, −NH−CH_2−**CH_2**−O−), 3.50 (t, 176 H, −CH_2−**CH_2**−O−), 4.47−4.65 (m, 1H, −NH−**CH**(CO−)−CH_2−).

The degree of derivatization with PEG_{2000} chains ($DD_{PEG2000}$) was determined by ^{1}H NMR in DMSO-d_6 and calculated by comparing the integral of the peak related to protons at 3.50 δ −(CH_2−**CH_2**−O)$_n$− (belonging to PEG_{2000}) with the integral related to protons at 3.12 δ awardable to −NH−**CH_2**−CH_2−O− (belonging to PHEA). The $DD_{PEG2000}$ was expressed as mean value of three determinations and was 7.0 ± 0.5 mol %. The $\bar{M}_w$ of PHEA-PEG_{2000}, determined by SEC analysis, was 68.7 kDa ($\bar{M}_w/\bar{M}_n$ = 1.95).

PHM-PEG_{2000} Synthesis. Derivatization of PHEA-PEG_{2000} ($DD_{PEG2000}$ = 7 ± 0.5 mol %) with methacrylic anhydride to obtain PHM-PEG_{2000} copolymer was carried out according to the following procedure: PHEA-PEG_{2000} (50 mg/mL) was dissolved in anhydrous DMA, and then a suitable amount of TEA and MA were added, according to $R_1 = R_2$ = 0.4, 0.5, or 1.0. The reaction was kept at 40 °C under continuous stirring for 48 h. After this time, the reaction mixture was precipitated in 2-propanol and centrifuged for 10 min, at 11 800 rpm and 4 °C. The product was recovered, washed several times with 2-propanol and acetone, and then dried under vacuum.

FT-IR spectrum (KBr) of PHM-PEG_{2000} showed a broad band centered at 3300 cm^{-1} (asymmetric stretching O−H and N−H); bands at 2917 (stretching C−H); 1717 (asymmetric stretching COO); 1656 (amide I); 1543 (amide II), 1300 (scissoring =C−H), 1170 (symmetric stretching COO), and 1110 cm^{-1} (stretching C−O).

The ^{1}H NMR spectrum (D_2O) showed δ 1.90 (s, 3H, −CO−C(**CH_3**)=CH_2), 2.80 (m, 2H, −CH−**CH_2**−CO−NH−), 3.35 (t, 2H, −NH−**CH_2**−CH_2−O-), 3.64 (t, 2H, −NH−CH_2−**CH_2**−O−), 3.71 (t, 176 H, −CH_2−**CH_2**−O-), 4.75 (m, 1H, −NH−**CH**(CO−)−CH_2−), 5.71, and 6.12 (2s, 2H, −CO−C(CH_3)=**CH_2**).

The degree of derivatization in methacrylic groups (DD_{MA}) was determined by ^{1}H NMR in D_2O by comparing the integral of the peaks related to protons at 1.9 δ as well as to protons between 5.71 and 6.12 δ respectively awardable to −CO−C(**CH_3**)=CH_2 and −CO−C(CH_3)=**CH_2** (belonging to linked methacrylic residues) with the integral related to protons at 2.80 δ awardable to −CH−**CH_2**−CO−NH− (belonging to PHEA) and expressed as mean value of three determinations.

Preparation of PHM Nanoparticles (Sample A) and PHM/PHM-PEG_{2000} Nanoparticles (Samples B−D). In a typical experiment, 15 mL of the organic phase, prepared by mixing 45.6 g of EtOAc (ρ = 0.902) with 39.7 g of PC (ρ = 1.189) and saturated with twice-distilled water before using (0.65 g/mL), was placed in a round-bottomed cylindrical glass reaction vessel fitted with an Ultraturrax and then treated with 0.5 mL of the aqueous phase. The aqueous internal phase was prepared dissolving a proper amount of copolymers (total copolymer aqueous concentration equal to 60 mg/mL) in twice-distilled water, previously saturated with the organic phase. In particular, sample A was obtained by using PHM alone, whereas samples B−D were obtained using a mixture of PHM/PHM-PEG_{2000} at 15, 30, and 50% of PHM-PEG_{2000} copolymer weight on the total copolymer amount, respectively.

Then the mixture was treated with the proper amount of Synperonic L61 (range 0.3−1.2% w/v) and stirred at 8000 rpm for 15 min. The obtained microemulsion was placed in quartz tubes, each equipped with an internal quartz piston in order to have about 2 mm in thickness of sample and then irradiated at 254 nm for 1.5 h.

The absence of irradiation effects on PC and on the PC/EtOAc mixture under used irradiation condition was already demonstrated.[10]

After the irradiation process, samples were centrifuged at 15 000 rpm at 4 ± 0.1 °C for 30 min in order to separate nanoparticles from the organic phase. Then nanoparticles were purified by several washings with distilled water and centrifuged from time to time at 15 000 rpm at 4 ± 0.1 °C for 1 h. Finally, nanoparticle samples were washed with acetone and dried under vacuum until weights remain constant.

Particle Size Determination. The average diameter and width of distribution (polidispersity index, PDI) of A−D nanoparticle samples were determined by photon correlation spectroscopy (PCS), at the temperature of 25 ± 0.1 °C and by using twice-distilled water as suspending medium. The suspension, properly diluted with filtered (0.2 μm) twice-distilled water, was kept in a cuvette and analyzed. Particle size distribution was determined by using an algorithm based on the non-negative least squares (NNLS) method.

Zeta Potential Measurements. Zeta potentials of A−D nanoparticle samples were measured by dispersion of each dried nanoparticle batch in a filtered (0.2 μm) twice-distilled water, phosphate buffer at pH 7.4, or aqueous NaCl 0.9 wt % solution as dispersing media.

XPS Analysis. The surface chemical composition of the samples was studied by XPS in an ultrahigh vacuum (UHV) chamber with a base pressure in the range of 10^{-8} Torr during data collection. The binding energy (BE) scale was calibrated by measuring C 1s peak (BE = 285.1 eV) from the surface contamination. Measurements were recorded with an accuracy of ±0.1 eV. Relative concentrations of chemical elements were calculated by a standard quantification routine, including Wagner's energy dependence of attenuation length and a standard set of VG Escalab sensitivity factors.[15] A nonlinear least-squares peak fitting routine was used for spectra analysis, separation elemental species in different chemical environments.

Transmission Electron Microscopy (TEM). Dried nanoparticle samples were dispersed directly into twice-distilled water, and then a copper grid coated with carbon film was put into the above suspension several times. After being stained by phosphotungstic acid solution (2 wt %) and dried at room temperature, samples were ready for the TEM investigation. Observation was performed at an accelerating voltage of 100 kV.

Swelling Studies. The swelling ability of polymeric nanoparticles was determined at 37 ± 0.1 °C in twice-distilled water, HCl 0.1 N (pH 1), and phosphate buffer (NaCl, Na_2HPO_4, and KH_2PO_4) at pH 6.8 and 7.4. In particular, accurately weighted aliquots of the dried sample (15 mg) were kept into contact with penetrating medium (2 mL) until the equilibrium swelling was reached (24 h); then each swollen sample was filtered, plugged by blotting paper and weighed. The weight swelling ratio was calculated as follows:

$$q = W_s/W_d$$

where W_s and W_d are the weights of swollen and dry sample, respectively. Every experiment was performed in triplicate.

Chemical Stability. Chemical stability of samples was investigated in HCl 0.1 N (pH 1), phosphate buffer solution at pH 6.8 and 7.4 (NaCl, Na_2HPO_4, and KH_2PO_4). Samples (15 mg) were dispersed in 10 mL of liquid medium, then kept in a water bath at 37 ± 0.1 °C under continuous stirring (100 rpm) for 2 h at pH 1 and 24 h at pH 6.8 and 7.4. After this time, samples were neutralized (when necessary) and centrifuged at 15 000 rpm at 10 °C for 15 min, and the supernatant was separated. For each sample, remaining nanoparticles were washed five times with distilled water under continuous stirring at 37 ± 0.1 °C for 1 h to extract some soluble polymer chain and electrolytes remained inside the network. Finally, the remaining samples were washed with acetone and centrifuged at 15 000 rpm at 10 °C for 15 min. The recovered solid residue was dried, weighed, and characterized by FT-IR analysis and swelling studies in twice-distilled water.

Enzymatic Stability. Accurately weighted aliquots of nanoparticles (15 mg) were incubated under continuous stirring (100 rpm) at 37 ± 0.1 °C in (a) 2 mL HCl solution (0.01 N) at pH 2 containing pepsin (final enzyme concentration = 0.6 mg/mL) for 24 h; (b) 2 mL of TRIS buffer 0.08 M solution at pH 8 containing $CaCl_2$ 0.1 M and α-chymotrypsin (final enzyme concentration = 0.6 mg/mL) for 24 h; (c) 2 mL of phosphate buffer solution (NaCl, Na_2HPO_4, and KH_2PO_4) containing esterase (final enzyme concentration = 0.5 mg/mL) for 24,

48, and 72 h. For the experiments carried out in the presence of esterase, a new dose of enzyme was added after each 24 h. After each experiment, samples were purified and characterized by the same procedure used for samples subjected to chemical stability studies. The same experiments were carried out in the absence of enzymes as control.

Cell Viability Assay. Cell compatibility of nanoparticles was tested in vitro by using human chronic myelogenous leukemia (K-562) cell line and the Trypan blue exclusion assay. Cells were suspended at a density of 1×10^5 cells mL^{-1} in RPMI-1640 medium (supplemented with 10 vol % of fetal calf serum, 2 mmol/L L-glutamine, 100 U/mL penicillin, and 100 g/mL streptomycin) (Sigma Aldrich, Italy), transferred to 24-well plate (1 mL for well) and incubated at 37 °C in a humidified atmosphere containing 5% of CO_2, in the presence of A−D samples (four well condition) at three different final concentrations (0.5, 1.0, and 2.5 mg/mL) for 48 h. After this time, 100 μL of each suspension (containing cells and nanoparticles) were diluted (1:1) and colored with Trypan blue solution (0.4 wt %). The viable cells number was calculated in a hematocytometer by dye exclusion, and the viability was expressed as a percentage of the uncolored cells in comparison with total cells. In the control experiment, cells were incubated in the suspending medium in the absence of nanoparticles.

Preparation of Fluorescein-Loaded Nanoparticles. Fluorescein-loaded nanoparticles were obtained by using as internal phase of the microemulsion a fluorescein sodium salt solution in twice-distilled water (4 mg/mL) and using the same copolymer weight ratios as the nanoparticles without fluorescein. A_F−D_F nanoparticle samples were so obtained.

Culture of Macrophages and Fluorescein-Loaded Nanoparticle Uptake. Phagocyte uptake of A_F−D_F nanoparticle samples was determined by using mouse monocyte macrophage cell line (J774 A.1).

Cells were routinely cultured at 37 °C in a humidified atmosphere with 5% CO_2, in 25 cm^2 flasks containing 10 mL of Minimum Essential Medium Eagle (MEME; Sigma Aldrich, Italy) supplemented with 10 vol % fetal bovine serum (FBS), antibiotics (2.5 μg/mL Amphotericin B, 100 U/mL penicillin, and 100 μg/mL Streptomycin) (Sigma Aldrich, Italy). The medium was changed every third day.

To study cellular uptake of A_F−D_F fluorescein-loaded nanoparticle samples via fluorescence microscopy, cells were suspended at a density of 4×10^5 cells mL^{-1} in MEME supplemented with FSB and antibiotics, transferred to 24-well plate (1 mL for well) and incubated at 37 °C in atmosphere containing 5% CO_2 for 24 h.

After this time, macrophages were washed with RPMI1640 medium without supplements in order to remove nonadherent cells. Adherent cells were further incubated in MEME enriched with FBS and antibiotics for 24 h. At the end of this incubation time, 100 μL of aqueous suspension (27.5 mg mL^{-1}) of samples A_F, B_F, C_F, or D_F were added (four well condition). Further 100 μL of fluorescein aqueous solution (1.6 mg mL^{-1}) was added in four wells in order to evaluate the phagocytosis of free dye. Moreover, four wells were added of 100 μL of twice-distilled water and used as control. The culture plate was incubated for 8 h.

After this time, macrophages were washed and rinsed twice with MEME without supplements in order to remove the nonphagocytized particles. Then, to each well was added 100 μL of MEME, and the bottom of each well was scraped in order to peel off adherent cells. A drop of cell suspension was put on a slide and viewed by a fluorescence microscope.

Results and Discussion

In this paper, polymeric nanoparticles were obtained from acryloylated derivatives of PHEA, PHM, and PHM-PEG_{2000} copolymers by using the UV-irradiation method of an inverse microemulsion.[10]

Synthesis of PHM. PHEA-MA (PHM) was obtained by partial modification of PHEA with methacrylic anhydride (MA). This reaction of derivatization was carried out in anhydrous DMA using TEA as catalyst, in agreement with a previously reported procedure.[12] The degree of derivatization (DD_{MA}) of PHEA with MA, obtained under the used experimental conditions and determined by ^{1}H NMR (see the Experimental Section), was equal to 30 ± 1 mol %.

Synthesis of PHEA-PEG_{2000} and PHM-PEG_{2000}. The reaction between PHEA and PEG_{2000} amino-derivative, schematically reported in Scheme 1, was carried out in the presence of PNPC as activating agent.

The DD in PEG_{2000} ($DD_{PEG2000}$) evaluated from ^{1}H NMR spectrum of the copolymer in DMSO-d_6 (see Figure 1) was calculated by comparing the integral of the peak related to protons at 3.50 δ $-(CH_2-\mathbf{CH_2}-O)_n-$ (belonging to PEG_{2000}) with the integral related to protons at 3.12 δ awardable to $-NH-\mathbf{CH_2}-CH_2-O-$ (belonging to PHEA). The $DD_{PEG2000}$ was expressed as mean value of three determinations and resulted to be 7.0 ± 0.5 mol %.

The FT-IR spectrum of PHEA-PEG_{2000} showed a new peak relating to the presence of PEG moieties into its structure, such as the peak at 1110.0 cm^{-1}, attributed to the stretching of C−O, which is absent in the spectrum of the starting PHEA (see the Experimental Section). Also the SEC analysis of the obtained copolymer confirmed the introduction of PEG moieties on PHEA-PEG that shows a weight-average molecular weight ($\bar{M}_w$) of 68.7 kDa ($\bar{M}_w/\bar{M}_n = 1.95$). This $\bar{M}_w$ value was greater than of PHEA and quite in agreement with the theoretical one (based on the PEG_{2000} degree of derivatization).

To achieve photocrosslinkable PEGylated copolymers, PHEA-PEG_{2000} copolymer so obtained was subsequently kept to react with different amounts of MA and TEA obtaining PHEA-PEG_{2000}-MA (PHM-PEG_{2000}) copolymers at different degrees of derivatization in MA (DD_{MA}). Three different PHM-PEG_{2000} copolymers were obtained as reported in Table 1.

As expected, increasing MA as well as TEA amounts (R_1 and R_2) DD_{MA} increases. Besides, as DD_{MA} increases, the yield values slightly decreases. This is reasonable because increasing DD_{MA} also increases the organic solvent solubility of copolymers (like acetone), and a little loss of material can be determined by the acetone washing procedure.

Therefore, for the subsequent nanoparticle production, PHM-PEG_{2000} copolymer at DD_{MA} equal to 14 mol % was used. This copolymer was chosen either because it is easily soluble in the aqueous internal phase and not soluble in the organic external phase of the microemulsion and because it does not have too many photocrosslinkable groups that could give a too compact nanomatrix.

Preparation of PHM Nanoparticles (Sample A_1−A_5). For obtaining nanoparticles of PHM, a stable inverse microemulsion was prepared by mixing the aqueous phase containing the acryloylated copolymer (60 mg/mL) and the organic phase prepared by mixing EtOAc with PC ($R = 1/30$, where R is the aqueous/organic phase ratio).

A previous saturation of the organic phase and aqueous phase with each other was carried out in order to avoid diffusion processes between external and internal phases during the irradiation process.

The microemulsion was mixed at 8000 rpm for 15 min with an Ultraturrax system in the presence of Synperonic L61 as surfactant and subjected to an irradiation process using an UV source at 254 nm for 1.5 h. The UV irradiation provokes the cross-linking reaction between PHM chains inside each nanodrop and the consequent formation of nanoparticles (sample A).

In the first step of the work, the technological parameters for obtaining nanoparticles with the appropriate size were found.

Scheme 1. Schematic Representation of PHEA-PEG_{2000} Synthesis ($n = 44$)

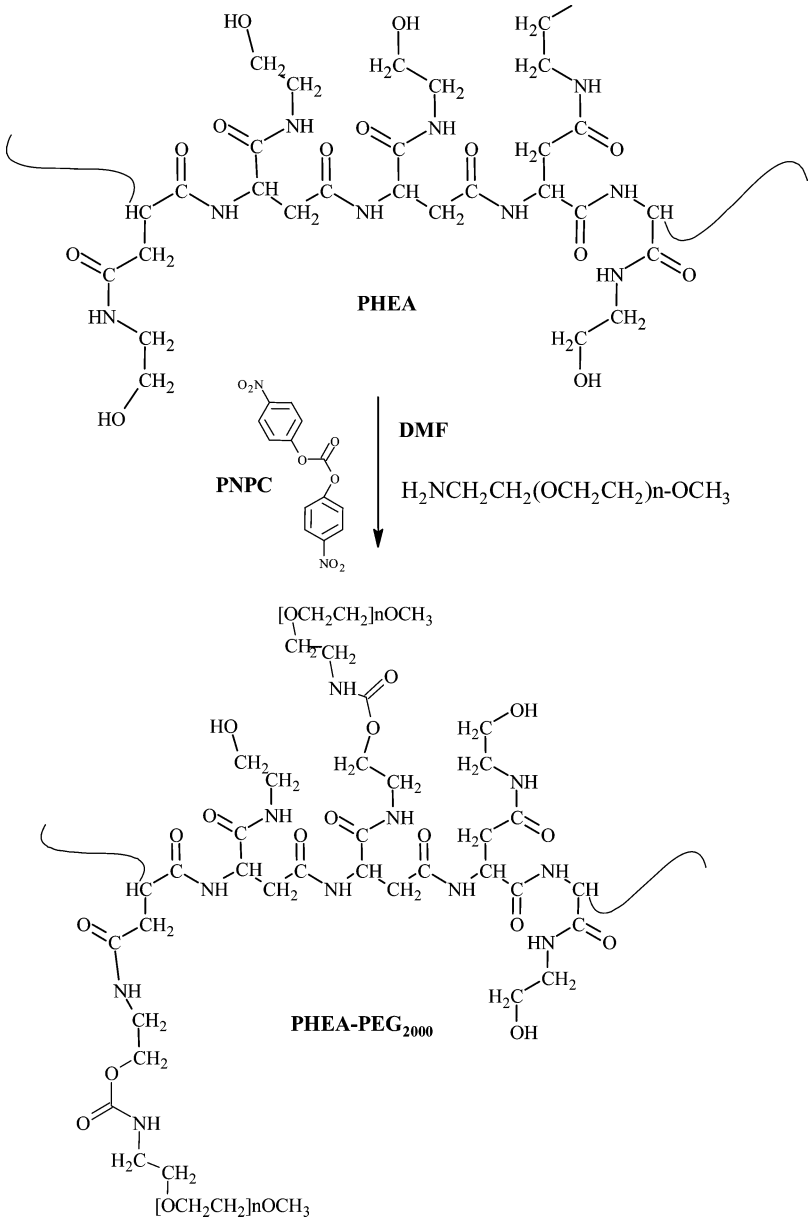

For this reason, the microemulsion was prepared using different amounts of surfactant in the range of 0.3−1.2% w/v (surfactant weight/organic phase volume).

In Table 2, PHM nanoparticle yields (wt.-%), mean diameter (nm), and PDI as a function of surfactant amount added for preparing the microemulsion are reported.

By using surfactant amounts lower than 0.6% w/v, the microemulsion was unstable during the irradiation process, whereas by using 0.6% w/v or higher synperonic amounts, an homogeneous and stable colloidal system was obtained. The smallest nanoparticles were obtained by using the greatest surfactant amounts in the range of 0.9−1.2% w/v; this is reasonable because a larger amount of surfactant stabilizes the microemulsion giving smaller nanodrops whose mean diameter was constant.

Moreover, a study on PHM nanoparticle size as a function of stirring rate of microemulsions before the irradiation process was carried out by fixing the amount of surfactant at 0.9% w/v. When the stirring rate was varied from 8000 to 20 500 rpm, no further size reduction was detected; for this reason, 8000 rpm was chosen in this work as the stirring rate for nanoparticle preparation.

Preparation of PHM/PHM-PEG_{2000} Nanoparticles (Samples B−D). With the purpose of obtaining potentially stealth nanoparticles that are able to escape the massive uptake from the reticulo-endothelial system (RES) after e.v. administration, a new PHEA copolymer was prepared containing in its structure covalently linked PEG chains and moieties bearing double bonds.

The possibility of using a copolymer bearing covalently linked PEG chains for preparing nanoparticles could provide many advantages in comparison with hydrophilic polymers just adsorbed on the nanoparticle surface, because of the absence of fast desorption of the hydrophilic coating after administration of these systems in the blood stream. This strategy is very important for giving particles with a long circulation half-life because this coating has the function of repelling plasma proteins avoiding the opsonisation process, which is responsible for the fast phagocytosis of nanoparticles by the RES.[16]

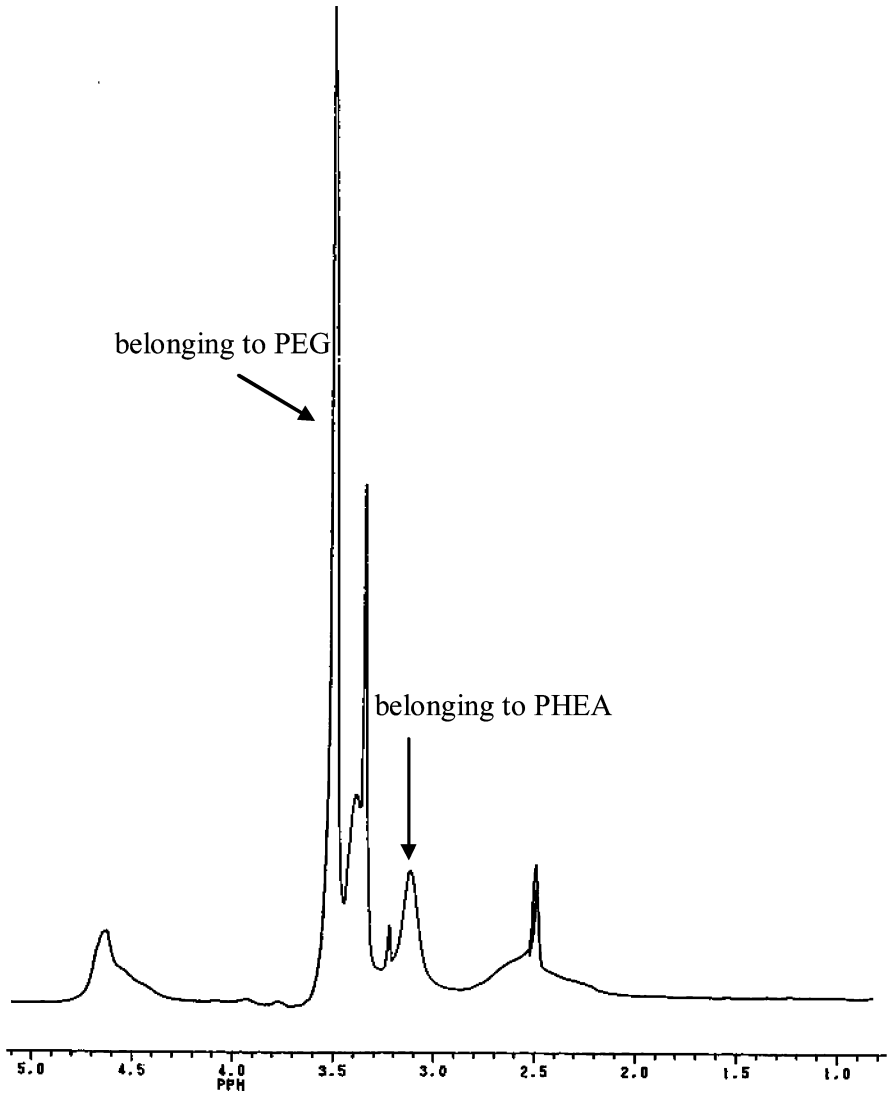

Figure 1. ^{1}H NMR spectrum of PHEA-PEG$_{2000}$ in DMSO-d_6.

Table 1. Yield Values and DD$_{MA}$ of PHM-PEG$_{2000}$ Copolymers (R_1= mol of MA/mol of PHEA Repeating Units; R_2 = mol of TEA/mol of MA)

R_1	R_2	yield (wt %)	DD$_{MA}$ (mol %)
0.4	0.4	91.0	14.0
0.5	0.5	86.6	19.0
1	1	84.8	36.4

In this study, a PHM-PEG$_{2000}$ copolymer with a DD$_{MA}$ equal to 14 ± 1 mol % (see Table 1) was chosen since it is easily soluble in the aqueous internal phase and not soluble in the organic external phase of the microemulsion and potentially have to give nanoparticles with a proper porosity. The $\bar{M}_w$ of this PHM-PEG$_{2000}$ copolymer determined by SEC measurements was 69.9 kDa ($\bar{M}_w/\bar{M}_n$ = 1.66).

Polymeric nanoparticles were prepared using as the aqueous phase of the microemulsion solutions of both PHM and PHM-PEG$_{2000}$ copolymers at different weight ratios.

The proper amounts of copolymers were dissolved in water, previously saturated with the organic phase. Then these solutions were used for preparing stable microemulsions by stirring at 8000 rpm for 15 min and using Synperonic at 0.9% w/v. After this time, each microemulsion was irradiated at 254 nm for 1.5 h.

Table 2. PHM Nanoparticle Yields (wt %), Mean Diameter (nm) and PDI as a Function of Surfactant Amount Added for Preparing the Microemulsion[a]

sample	Synperonic L61 (% w/v)	yield (wt %)	mean diameter (nm)	PDI
A$_1$	0.3	31.7	198.3	0.50
A$_2$	0.4	78.9	188.9	0.37
A$_3$	0.6	80.5	172.2	0.25
A$_4$	0.9	87.7	147.0	0.24
A$_5$	1.2	74.0	149.0	0.27

[a] The average size of nanoparticles was calculated in the range between 5 and 95 % for each sample.

Obtained nanoparticulate samples were expressed with a capital letter as a function of the ratio % of PHM-PEG$_{2000}$ copolymer weight on the total copolymer amount; therefore, nanoparticle samples at 15, 30, or 50 wt % of PHM-PEG$_{2000}$ were prepared and called B, C, and D samples, respectively.

Characterization of PHM and PHM/PHM-PEG$_{2000}$ Nanoparticles. All of the obtained nanoparticle samples were insoluble in water and in common organic solvents, such as dichloromethane, acetone, dimethyl sulfoxide, dimethylacetamide, and *N*,*N*′-dimethylformamide.

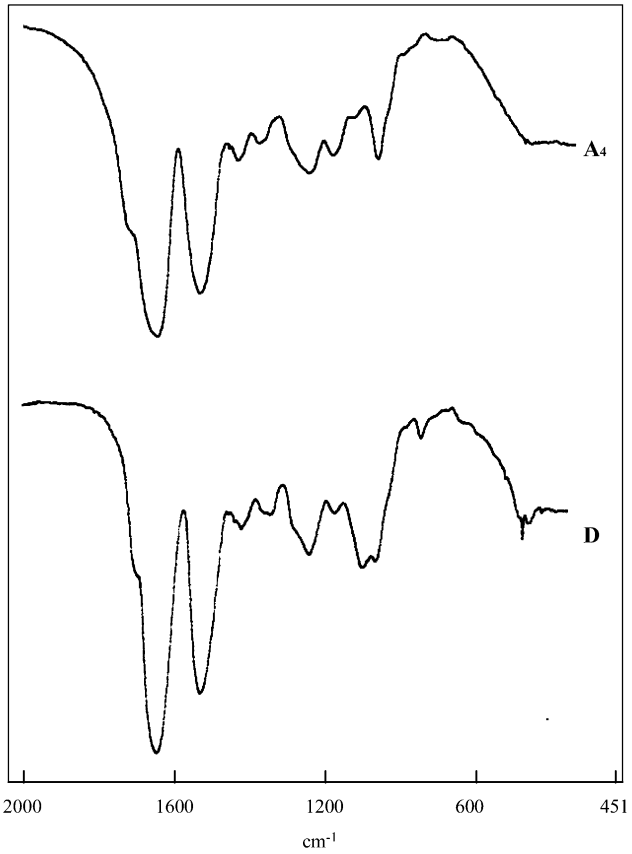

Figure 2. FT-IR spectra of nanoparticle samples A_4 and D. Spectra are recorded in transmittance scale (%*T*).

FT-IR spectra were carried out on A_1-A_5 and B−D samples. Spectra of samples A_4 and D are compared in Figure 2.

Both spectra showed the peak at 1730 cm^{-1}, which was attributed to the ester carbonyl asymmetric stretching, indicating the presence of these groups in the nanoparticles also after the irradiation process. This peak was also shifted to higher frequency (from 1720 to 1730 cm^{-1}), indicating the loss of the conjugation with the double bond of the methacrylic residue, which is responsible for the cross-linking reaction between the polymeric chains and that disappears as a consequence of the cross-linking process.

The spectrum of sample D showed a typical peak at 1110.0 cm^{-1} attributed to the C−O stretching of PEG moieties, which was absent in PHM nanoparticles (Figure 2, spectrum A). This peak had higher transmittance increasing the amount of PEG present as PHM-PEG_{2000} copolymer in the aqueous phase before the irradiation process going from sample B to D.

All samples (A_4, B, C, and D) were also characterized in terms of yield wt %, mean diameter, PDI, and zeta potential values in twice-distilled water; obtained values were reported in Table 3.

As can be seen, an increase in the amount percent of PHM-PEG_{2000} going from sample A_4 (without PHM-PEG_{2000}) to sample D (at 50 wt.-%) of PHM-PEG_{2000} mean diameter increased going from 147.0 to 237.5 nm, respectively. This result could be explained considering that going from sample A_4−D nanoparticles containing an increasing PEG amount were obtained with a lower cross-linking degree because of the minor amount of double bonds available. Therefore, when the PHM-PEG_{2000} content was increased, looser and larger nanomatrixes were obtained.

To estimate the efficiency of surface modification of nanoparticles with PEG moieties, zeta potential measurements were carried out; obtained values were reported in Table 3. As can be seen, a reduction of the surface charge of nanoparticles in water was observed as the PEG_{2000} amount increased from sample A_4 to D, probably because of its location mainly onto the nanoparticle surface.

Table 3. Yield (wt %), Mean Diameter (nm), PDI, and Zeta Potential in Twice-Distilled Water of A_4, B, C, and D Nanoparticle Samples[a]

sample	yield (wt %)	mean diameter (nm)	PDI	zeta potential (mV)
A_4	87.7 ± 1.5	147.0	0.24	−49.10 ± 6.05
B	91.0 ± 2.1	184.2	0.27	−19.63 ± 5.72
C	93.2 ± 1.2	189.6	0.25	−16.45 ± 4.32
D	91.4 ± 0.9	237.5	0.29	−15.86 ± 4.65

[a] Values are means ± s.d. ($n = 3$). The average size of nanoparticles was calculated in the range between 5 and 95 % for each sample.

Table 4. High-Resolution C 1s, O 1s, and N 1s Peak Quantitative Analysis of XPS on Surface of the Samples A_4, B, C, and D

sample	C 1s			O 1s		N 1s
BE (eV)	285.1 −C−C−	286.5 −C−O−	288.3 −C═O	531.5 −C−O−, −O−H	532.9 −C═O	399.9 −N−H
A_4	39.2	14.0	11.3	17.7	6.5	11.3
B	36.7	18.3	11.7	17.8	5.2	10.4
C	35.4	18.5	12.0	17.8	5.5	10.8
D	34.9	18.6	12.1	17.6	5.9	10.9

With the aim of investigating in detail the chemical composition of the nanoparticle surface, X-ray photoelectron spectroscopy analysis (XPS) was used to analyze samples A_4, B, C, and D. XPS is a surface-sensitive technique that gives information on the chemical composition and structure of the surface layer using the photoelectric effect.

In this technique, X-rays are directed at the sample, causing the electrons of surface atoms to be emitted from their orbitals. The element from that the electron originates, and the chemical environment of this element is given by the measured kinetic energy of the electrons. Only those electrons that leave the surface without energy loss will contribute to the peak signifying that element. Electrons that originate from far below the surface (i.e., >10 nm distance) suffer energy loss through collisions and are unable to leave the surface or they escape the surface with considerable energy loss.[17]

The binding energies (BE) of the main XPS peaks and the surface chemical composition of investigated samples were reported in Table 4 as a function of PEG amount into A_4−D samples. Elemental concentrations were expressed as atomic percentage (atom. %). A curve-fitting procedure was used to calculate the relative distribution of the carbon and oxygen species on the surface of the samples.

The C 1s core-level spectrum consists of three components: a major peak at BE = 285.1 eV that is assigned to C−C bonds; a peak at BE = 286.5 eV that is attributed to C−O bonds, and another component at BE = 288.3 eV, assigned to C═O bonds.[15] The O 1s core-level spectrum consists of two components: a peak at BE = 531.6 eV that is assigned to C−O bonds and hydroxyl groups (−OH) and another component at BE = 532.9 eV that is attributed to C═O bonds in carboxyl groups (RCOO−).[15]

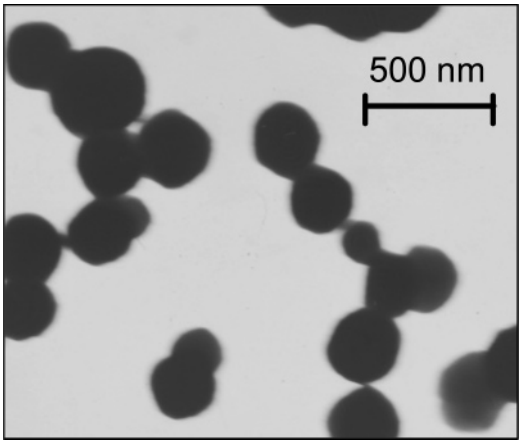

Figure 3. Transmission electron micrograph of sample D at a calibrated magnification of 40 000×.

Table 5. Weight Swelling Ratio (q) of A_4 and B−D Samples in Different Penetrant Media. Every Experiment Was Performed in Triplicate

	q			
	penetrating medium			
sample	distilled water	pH 1	PBS pH 6.8	PBS pH 7.4
A	10.2 ± 0.2	8.9 ± 0.1	8.9 ± 0.1	9.3 ± 0.1
B	11.3 ± 0.1	8.7 ± 0.1	8.6 ± 0.2	8.5 ± 0.2
C	10.9 ± 0.1	8.5 ± 0.2	8.2 ± 0.1	8.2 ± 0.1
D	10.0 ± 0.3	8.3 ± 0.3	7.6 ± 0.2	7.6 ± 0.3

From the analysis of these results, a decrease in both nitrogen atoms and in C−C bond amounts on the surface (becaming mainly from the polyaminoacidic backbone) and a distinct increase of C−O groups on the surface were detected from sample A_4 to D. This result was in agreement with a greater amount of PEG chains on the surface of nanoparticles.

Moreover, the percentage variation of the component at 531.5 eV cannot be useful because it includes both −C−O− and −OH oxygen species coming from either increasing PEG or decreasing PHM moieties on the surface, respectively.

A morphological characterization of A_4 and B−D nanoparticles was carried out. Figure 3 shows as an example a TEM photograph of sample D (50 wt % of PHM-PEG_{2000} nanoparticulate systems).

As can be evidenced by TEM, the obtained nanoparticles revealed a spherical shape, and mean diameter values are in good agreement with that obtained by PCS analysis; in particular, the mean diameter of the sample D was about 250 nm (vs 237.5 nm by PCS analysis).

Swelling Studies. To evaluate the affinity of A_4 and B−D samples toward aqueous media, swelling measurements were carried out in twice-distilled water at 37 °C for 24 h on dried samples. Swelling measurements were also performed in media at different pH values in order to simulate some biological fluids (simulated gastric and intestinal fluids at pH 1 for 2 h and then at pH 6.8 for 24 h as well as extracellular fluid at pH 7.4 for 24 h).

The weight swelling ratios (q) in different media calculated using $q = W_s/W_d$, where W_s and W_d are the weights of swollen and dry sample, respectively, were reported in Table 5.

Data showed that the weight swelling ratio values of all the samples investigated resulted slightly affected by the osmotic pressure and ionic strength but not affected from the pH value of the used penetrating media. However, the amount of water soaked up from the nanoparticles is quite low. For this reason, no significant differences in q values were evidenced as the sample cross-linking degree decreases (increasing PEG amount going from samples A to D).

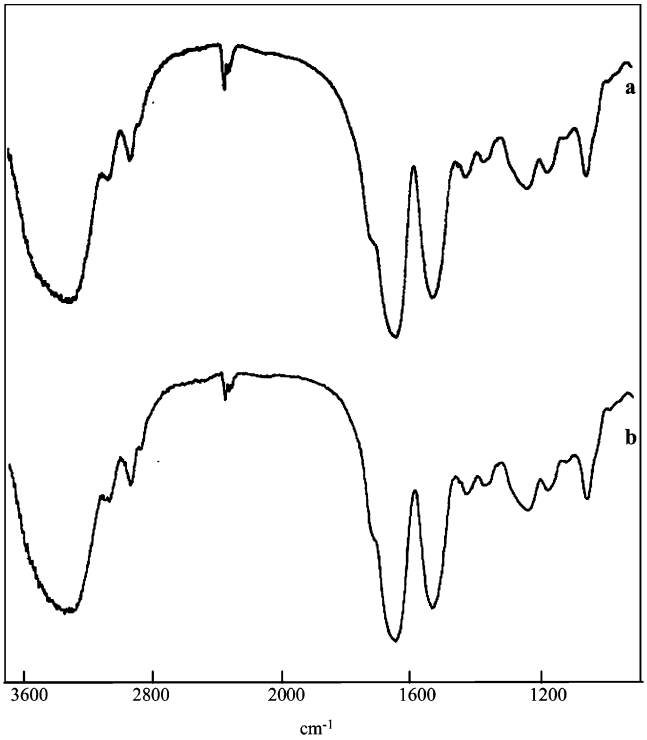

Figure 4. FT-IR spectra of nanoparticle sample A_4 before (a) and after (b) chemical treatment at pH 1. Spectra are recorded in transmittance scale (%*T*).

This properties could be successfully exploited to plan the direct administration of these nanosystems in the blood stream since also in the swollen form at physiological pH these systems are nanosized (see Table 3).

Chemical and Enzymatic Stability. Because of the presence of chemically degradable bonds in the structure of A_4 and B−D samples (i.e., ester groups), their stability after some chemical treatments was investigated. In particular, the chemical stability of the samples was evaluated by incubating them in HCl (pH 1) solution at 37 ± 0.1 °C for 2 h and phosphate buffer (pH 6.8 and 7.4) solutions at 37 ± 0.1 °C for 24 h.

No degradation of the nanostructure of samples was detected during the time interval chosen for this investigation due to the chemical treatment, as evidenced by the high yields of samples and the swelling ratio values, calculated in twice-distilled water (data not reported), that were comparable with those obtained with starting samples (before the treatment).

The confirmation of the absence of degradation after chemical treatment was obtained by the FT-IR analysis of all the samples (data not showed). In Figure 4, the FT-IR spectrum of sample A_4 before and after the chemical treatment at pH 1 was reported. In fact, intensities (transmittance %) and positions of bands of chemically treated samples remained unmodified in comparison with the untreated one.

To evaluate the possibility to administer these systems by the oral route, the stability of all of the samples toward the gastro-intestinal enzymes was evaluated in the presence of pepsin and α-chymotrypsin for 24 h. After this time, the percent residual weight of treated samples was determined, and the values of q of these residues were measured in twice-distilled water (see Table 6).

Results suggest a weak action of pepsin and chymotrypsin on all nanoparticles. FT-IR analysis on samples treated with

Table 6. Yield (wt %) after Enzymatic Treatment with Pepsin and α-Chymotrypsin of A_4 and B−D Nanoparticle Samples[a]

	sample			
	A_4	B	C	D
Yield (wt %)				
incubated with pepsin	97.5	97.7	96.8	97.2
incubated with α-chymotrypsin	98.2	96.4	98.5	98.0
q				
incubated with pepsin	9.8	10.3	10.6	10.2
incubated with α-chymotrypsin	10.4	10.7	11.2	11.0

[a] Every experiment was performed in triplicate and results were in agreement within ±2 % error.

Table 7. Yield (wt %) after Enzymatic Treatment with Esterase of A_4 and B−D Nanoparticle Samples[a]

time incubation with esterase	yield (wt%) sample			
	A_4	B	C	D
24 h	97.3	98.5	98.9	97.8
48 h	96.0	94.2	95.3	94.9
72 h	95.8	93.3	94.8	92.7

[a] Every experiment was performed in triplicate and results were in agreement within ±2 % error.

these enzymes also revealed no significant differences in comparison with untreated samples (data not shown).

This behavior could be properly exploited for the oral administration of drugs. In fact, the low swelling and degradability of these systems could improve the release of a loaded drug in the gastro-intestinal tract; besides these systems could reach the small intestine quite intact and here be adsorbed by lymphatic uptake via Peyer's patches thus reaching blood circulation.

Owing to the presence of ester bonds in the nanomatrixes, a detailed study on enzymatic stability in the presence of esterase was performed on all of the samples as a function of the incubation time, in particular for 24, 48, and 72 h. The yield of the residual nanoparticles recovered after each time of incubation with esterase was reported in Table 7; moreover their swelling ability in twice-distilled water as a function of incubation time was reported in Figure 5. These last data were considered as measurements of the progressive degradation by esterase, considering that, with increasing degradation, a greater number of small pieces of matrix interact with penetrating medium and swell absorbing water.

From data analysis, a partial progressive degradation of the matrix was evidenced as a function of incubation time, reasonably onto the particle surface and as a function of PEG content of samples. In fact, a reduction of the yield wt % and increases of *q* values of samples (see Table 7 and Figure 5) are evidenced from sample A_4 to D, mainly after 48 and 72 h of incubation.

This behavior could be important for the successful performance of these drug delivery systems. In fact, once in the blood stream, these systems will remain quite stable for 24 h, and they will start to be significantly degraded by esterase in the subsequent time. In this way, nanoparticles could have enough time to reach tissues, organs, or cells and here be degraded releasing drug molecules.

Cell Viability Assay. To investigate the effect of obtained nanoparticles on cell viability, various concentrations of nanoparticles (0.5, 1, and 2.5 mg/mL) were kept in contact with the K-562 cell line (human chronic myelogenous leukaemia). In particular, cell viability was evaluated by the Trypan blue exclusion assay, considering that, after incubating with test samples, cells with damaged membranes will be colored by the dye. In Figure 6, cell viability in the presence of three different amounts of samples A_4, B, and D was reported.

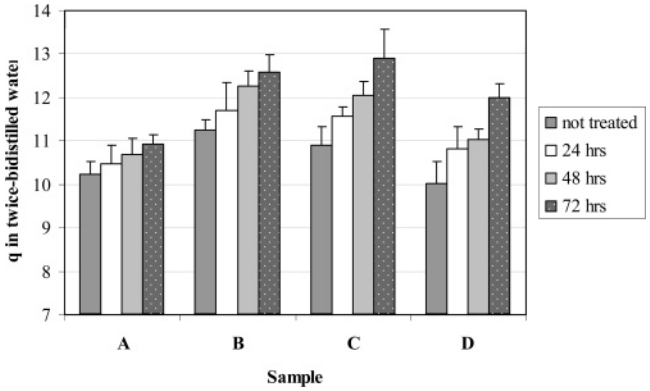

Figure 5. Swelling ratio values in twice-distilled water of A_4 and B−D samples after enzymatic treatment with esterase as a function of the incubation time.

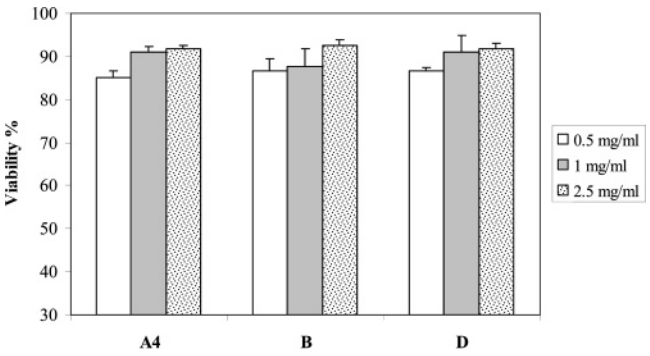

Figure 6. Viability (%) of K-562 cell line after 48 h of incubation with A_4, B, and D as a function of nanoparticle amount. Viability of cells in culture medium without nanoparticles was considered 100% (control).

As can be seen for all of the samples and at all of the amounts used (2.5, 1, and 0.5 mg/mL), values of growth inhibition were less than 15%. These data suggest that no significant cytotoxic effects on cells was evidenced at any used conditions.

Culture of Macrophages and Nanoparticle Phagocytosis. In order to evaluate the efficacy of surface PEG chains onto nanoparticles to make them able to escape the phagocytosis process, a study on fluorescein-loaded nanoparticle uptake by macrophages was carried out as a function of surface PEGylation degree.

Cells (mouse monocyte macrophages, J774 A.1) were grown in a proper medium containing 2.5 mg/mL of A_{4F}, B_F, C_F, or D_F nanoparticle sample for 8 h.

Figure 7 show phase contrast and fluorescence photographs of macrophages incubated with free fluorescein (image a) and fluorescein-loaded nanoparticle samples (images b−e).

Experimental data evidenced a significantly different behavior in phagocytosis of tested samples. In the presence of free fluorescein, cells appeared strongly and homogeneously green because of the free diffusion of fluorescein inside of the cell (image a). Cells incubated with sample A_{4F} (image b) showed inside several green small spots, indicating the presence of nanoparticles. In the case of sample B_F (image c), the nanoparticle uptake by macrophages decreased greatly if compared to sample A_F. For both samples C_F and D_F (images d and e), no uptake from macrophages was observed. This fact could be reasonably attributed to the presence of increasing PEG on the nanoparticle surface coming from B_F to D_F samples that make

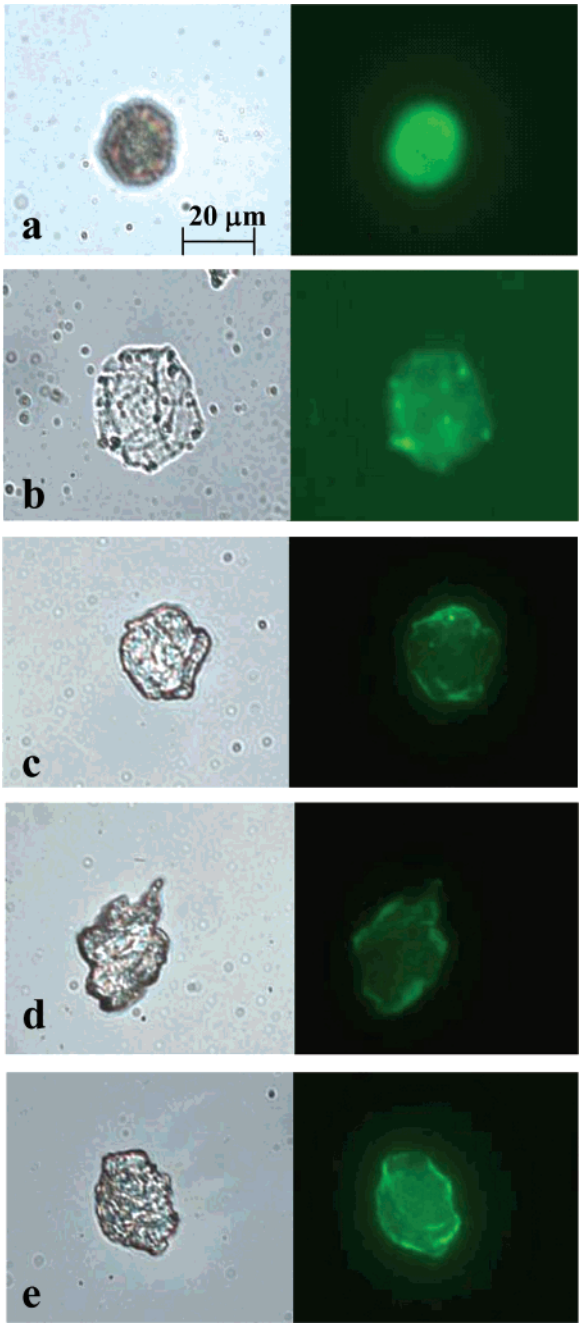

Figure 7. Phase contrast and fluorescence photographs of J774 A.1 cells after 8 h of incubation in the presence of (a) fluorescein aqueous solution, (b) sample A_{4F}, (c) sample B_F, (d) sample C_F, and (e) sample D_F.

them less sensible to the adsorption of proteins from the cultured medium increasing macrophage uptake.

Conclusions

The present paper describes the synthesis and the characterization of polymeric nanoparticles with a different surface PEGylation degree.

The starting polyaminoacidic material, PHEA, was functionalized with a PEG_{2000} amino-derivative, obtaining PHEA-PEG_{2000} copolymer. Both PHEA and PHEA-PEG_{2000} were subsequently derivatized with methacrylic anhydride (MA) in order to obtain PHM and PHM-PEG_{2000} copolymers, respectively, easily photocrosslinkable by an UV source. A process of UV irradiation of an inverse microemulsion, containing as internal phase an aqueous solution of different amounts of both copolymers, was used for obtaining nanoparticle samples with a different surface PEGylation degree. Obtained nanoparticles ranged in size from 147 to 240 nm. FT-IR analysis confirmed the introduction of PEG moieties in B−D samples. XPS investigations and zeta potential measurements confirmed the presence of PEG moieties mainly onto the nanoparticle surface. A significant affinity toward aqueous media of all of the obtained systems was found, slightly affected by the osmotic pressure and ionic strength of the used media. Studies for investigating the potential degradation of nanoparticles showed the absence of chemical degradation at several pHs and enzymatic degradation in the presence of enzymes of the gastro-intestinal tract. In the presence of esterase, the systems are slowly degraded as a function of time and depending on their surface PEGylation degree. Moreover, in vitro viability assays have also demonstrated that all of these systems did not have cytotoxic effects against the K-562 cell line under the used experimental conditions. Finally, in vitro studies on nanoparticle uptake by cell line J774 A.1 demonstrated the stealth properties of surface-PEGylated nanoparticles and identified samples B and D as having optimal biological behavior and encouraging their potential use as drug carriers for parenteral administration.

Acknowledgment. The authors thank Dr. Casaletto Maria Pia (ISMN, Sezione di Palermo, CNR, Italy) for the XPS analysis. The authors thank MIUR-FIRB for funding.

References and Notes

(1) Brigger, I.; Dubernet, C.; Couvreur, P. *Adv. Drug Delivery Rev.* **2002**, *54*, 631−651.
(2) Paolino, D.; Iannone, M.; Cardile, V.; Renis, M.; Puglisi, G.; Rotiroti, D.; Fresta, M. *J. Pharm. Sci.* **2004**, *93*, 1815−1827.
(3) Brannon-Peppas, L.; Blanchette, J. O. *Adv. Drug Delivery Rev.* **2004**, *56*, 1649−1659.
(4) Jagur-Grodzinski, J. *J. React. Funct. Polym.* **1999**, *39*, 99−138.
(5) Ahsan, F.; Rivas, I. P.; Khan, M. A.; Torres Suarez, A. I. *J. Controlled Release* **2002**, *79*, 29−40.
(6) Storm, G.; Belliot, S. O.; Daemen, T.; Lasic, D. *Adv. Drug Delivery Rev.* **1995**, *17*, 31−48.
(7) Owens, D. E., III.; Peppas, N. A. *Int. J. Pharm.* **2006**, *307*, 93−102.
(8) Harper, G. R.; Davies, M. C.; Davis, S. S.; Tadros, T. F.; Taylor, D. C.; Irving, M. P.; Waters, J. A. *Biomaterials* **1991**, *12*, 695−704.
(9) Dunn, S. E.; Brindley, A.; Davis, S. S.; Davies, M. C.; Illum, L. *Pharm. Res.* **1994**, *11*, 1016−1022.
(10) Craparo, E. F.; Cavallaro, G.; Bond, M. L.; Giammona, G. *Macromol. Chem. Phys.* **2004**, *205*, 1955−1964.
(11) Nakayama, Y.; Matsuda, T. *J. Polym. Sci.* **1992**, *30*, 2451−2457.
(12) Mandracchia, D.; Pitarresi, G.; Palumbo, F. S.; Carlisi, B.; Giammona, G. *Biomacromolecules* **2004**, *5*, 1973−1982.
(13) Giammona, G.; Tomarchio, V.; Pitarresi, G.; Cavallaro, G. *Polymer* **1997**, *38*, 3315−3323.
(14) Giammona, G.; Carlisi, B.; Palazzo, S. *J. Polym. Sci., Polym. Chem. Ed.* **1987**, *25*, 2813−2818.
(15) Moulder, J. F.; Stickle, W. F.; Sobol, P. E.; Bomben, K. D. In *Handbook of X-ray Photoelectron Spectroscopy*; Chastain, J., King, R. C., Jr., Eds.; Phys. Electronics Inc.: Eden Prairie, MN, 1995; pp 252−270.
(16) Moghimi, S. M.; Hunter, A. C.; Murray, J. C. *Pharmacol. Rev.* **2001**, *53*, 283−318.
(17) Sherwood, M. A. Data analysis in X-ray photoelectron spectroscopy. In *Practical Surface Analysis*, 2nd ed.; Briggs, D., Seah, M. P., Eds.; Wiley: New York 1990; pp 555−586.

BM060570C